coatings

MDPI

Article

Wastepaper Sludge Ash and Acid Tar as Activated Filler Aggregates for Stone Mastic Asphalt

Volodymyr Gunka [1,2,*], Volodymyr Hidei [2], Iurii Sidun [2], Yuriy Demchuk [1,3,*], Vitalii Stadnik [1], Pavlo Shapoval [1], Khrystyna Sobol [2], Nataliya Vytrykush [4] and Michael Bratychak [1]

1 Institute of Chemistry and Chemical Technology, Lviv Polytechnic National University, 12 Bandera Street, 79013 Lviv, Ukraine; vitalii.y.stadnik@lpnu.ua (V.S.); pavlo.y.shapoval@lpnu.ua (P.S.); mykhailo.m.bratychak@lpnu.ua (M.B.)
2 Institute of Civil Engineering and Building Systems, Lviv Polytechnic National University, 12 Bandera Street, 79013 Lviv, Ukraine; volodymyr.v.hidei@lpnu.ua (V.H.); yurii.v.sidun@lpnu.ua (I.S.); khrystyna.s.sobol@lpnu.ua (K.S.)
3 Department of General, Bioinorganic, Physical and Colloidal Chemistry, Danylo Halytsky Lviv National Medical University, 69 Pekarska Street, 79010 Lviv, Ukraine
4 Viacheslav Chornovil Institute of Sustainable Development, Lviv Polytechnic National University, 12 Bandera Street, 79013 Lviv, Ukraine; nataliya.m.vytrykush@lpnu.ua
* Correspondence: volodymyr.m.hunka@lpnu.ua (V.G.); yuriy_demchuk@ukr.net (Y.D.)

Abstract: Nowadays, the most common ways to dispose of acid tars and paper production waste are burial or incineration, but it is ecologically and economically expedient to use such waste in building materials. A new variant of filler aggregate—wastepaper sludge ash (paper production waste) and a chemical activator for filler aggregates—acid tar (oil-refining industry waste) is proposed. Elemental and mineralogical compositions of wastepaper sludge ash for comparison with commodity limestone mineral powder are established. Chemical activation of wastepaper sludge ash and limestone mineral powder was carried out and the wetting properties of the obtained materials were investigated by means of primary and neutralized acid tar. The physical and mechanical properties of stone mastic asphalt samples with different filler aggregate variants were studied. The possible chemical transformations in stone mastic asphalt using limestone mineral powder and wastepaper sludge ash activated by acid tar are shown. The possibility of replacing traditional limestone mineral powder with industrial wastepaper sludge ash has been proven, and the effectiveness of activating filler aggregates by acid tar has been confirmed. It was established that acid tar as an activator for filler aggregates does not require neutralization because stone mastic asphalt, in this case, demonstrates better properties compared to acid tar neutralization. As a result of our research, the application of wastepaper sludge ash is possible as a filler aggregate for stone mastic asphalt. And to obtain improved stone mastic asphalt characteristics, wastepaper sludge ash is required to activate 5 wt.% acid tar.

Keywords: filler aggregate; limestone mineral powder; wastepaper sludge ash; acid tar; stone mastic asphalt

Citation: Gunka, V.; Hidei, V.; Sidun, I.; Demchuk, Y.; Stadnik, V.; Shapoval, P.; Sobol, K.; Vytrykush, N.; Bratychak, M. Wastepaper Sludge Ash and Acid Tar as Activated Filler Aggregates for Stone Mastic Asphalt. *Coatings* **2023**, *13*, 1183. https://doi.org/10.3390/coatings13071183

Academic Editors: Qiao Dong and Valeria Vignali

Received: 15 April 2023
Revised: 31 May 2023
Accepted: 27 June 2023
Published: 30 June 2023

1. Introduction

Production of high-quality hot asphalt concrete mix is impossible without the application of a carefully selected, finely ground filler fraction of less than 0.063 mm. This asphalt concrete component should perform the following functions due to the presence of a large specific surface area (filler aggregate should be 90%–95% of the total surface area of grains that are part of asphalt concrete): increase the number of contacts between asphalt concrete structural components; fill small pores between asphalt concrete larger particles; and transfer bitumen from bulk state to film, forming from bitumen asphalt binder–mastic binding (asphalt binder–mastic). The most common variant of filler aggregate in the world that performs the described functions is mineral powder (MP) from the

main carbonate sedimentary rocks (limestone, dolomites, dolomitized limestone, and their varieties) containing calcium carbonate ($CaCO_3$) depending on the following categories: more than 70 (CC_{70}), more than 80 (CC_{80}), or more than 90 (CC_{90}) wt.%. The category is chosen depending on the used asphalt concrete mix and such external parameters as traffic intensity, pavement traffic load, climatic factors, and surface texture and traffic noise emissions [1–9].

MP absorbs a significant part of petroleum bitumen due to the high adsorbing surface, thus giving asphalt concrete the necessary characteristics: mechanical strength and resistance to deformation, which significantly improves the road surface quality and increases its service life. This significantly improves the quality of the resulting asphalt concrete, and the entire future road surface.

Many researchers [9–20] suggest the application other filler aggregate options, such as cement or waste cement dust, various types of ash and slag, gabbro, trachybasalt, quartz sandstone, rocks from postglacial deposits, activated carbon powder, sugar industry waste materials, and many others.

Industrial by-products containing combustible residues are used as alternative fuel. Wastes from paper sludge (PS) also belong to them. Currently, this waste in the form of wet sludge is mostly stored in dumps, which initiates the problem of disposal and environmental pollution. Partly after drying, this waste is used in road construction to consolidate the soil, in the ceramic industry, and in agriculture. It is also incinerated, forming the so-called wastepaper sludge ash (WSA).

Previous studies [21–23] have investigated the application of WSA as a substitute for traditional limestone mineral powder (LMP) in hot mix asphalt (HMA) preparation. It has been proven [21] that this material can completely or partially replace traditional LMP for HMA. As a result of replacing 50 wt.% of LMP with WSA, we obtain asphalt concrete material, which is not significantly inferior to the characteristics of asphalt concrete using LMP without foreign inclusions. Therefore, the task was to bring WSA to the conditional composition for the complete replacement of LMP in hot asphalt concrete without deterioration, and possibly with improvement in the properties of the latter. To carry this out, the authors proposed to activate WSA. As is known, depending on the formation mechanism of new active centers on the surface of the filler aggregate, activation is divided into the following categories: physical (mechanical activation); chemical; and physico-chemical. Mechanoactivation is based on the change in reactivity at the contact surface of mineral materials under the action of mechanical forces [24]. Mechanoactivation is carried out by a ball, drum, hammer, planetary, centrifugal shock, and jet mills [25].

Chemical activation methods [8,26–28] involve obtaining activated mineral powder (AMP) by adding activators to the raw material or to the crushed material, followed by grinding and mixing in mills. For activation by this method, cationic (higher aliphatic (fatty)) amines and aminoamides or their salts, as well as quaternary ammonium salts compounds) and anionic surfactants, such as higher carboxylic acids (synthetic fatty acids C_{17}-C_{20}, cubic residues of synthetic fatty acids), organic binders (bitumen and modified bitumen), bitumen plasticizers (tar and fuel oil, industrial oils, oils of vegetable industrial crops, some fuels), oligomers solutions (urea-formaldehyde resin, epoxy resins and polymer-containing wastes from epoxy resin production, rubber mainly with low molecular weight), inorganic substances (cement, slaked lime, various rocks), chemical reagents (calcium chloride solutions, salt solutions of iron, copper, and lead) are used.

The essence of physico-chemical activation is that the process of grinding raw materials is accompanied by the treatment of mineral powder with a mixture of bitumen and an activator. Moreover, the activator is injected at a time when the chemical activity of the newly formed surfaces is maximum.

In our case, the chemical activation of WSA by acid tar in pure (AT) and neutralized form (NAT) in a ball mill was chosen. AT was chosen as the activator because this by-product of oil refining technically belongs to the group of bitumen plasticizers, and ecologically, the problem of its utilization is not completely solved. In the refining industry,

sulfuric acid was used extensively as a reagent to purify unwanted components of distillate and residual oil fractions, paraffins, kerosene, and gasoline. Purification was performed to remove unsaturated hydrocarbons, sulfur- and nitrogen-containing compounds, and resinous compounds from oil fractions, the presence of which degrades the performance of petroleum products. As a result of this purification, sufficient amounts of AT were formed, which were not utilized but merged into the pits that are still used nowadays [29–33].

The authors hypothesized that the combined application of WSA and AT causes the formation of a qualitative AMP in which the concentration of active centers can increase by an average of 2.5–3 times. To test the effectiveness of the proposed new AMP, it was decided to design the composition of stone mastic asphalt (SMA) as the composition of this material requires high content of a mineral powder.

2. Experimental Section

2.1. Raw Materials

For the purpose of comparative testing, two filler aggregates were chosen for asphalt concrete: WSA of PJSC "Kyiv Cardboard and Paper Mill" and LMP produced by "Skala-Podilskii Spetscarier (Special Quarry)" (Skala-Podilska, Ukraine).

WSA was obtained as a result of incineration (combustion) in a fluidized bed at 850 °C PS according to [34]. In its original form, WSA consists of particles sized nearly 10 mm (Figure 1).

Figure 1. The appearance of WSA: (**a**) primary form; (**b**) crushed into a filler aggregate.

This material was ground using a ball mill to the fractions shown in Table 1. Also, for comparison, Table 1 shows the granulometric composition of the commercial LMP.

Table 1. Granulometric composition of the WSA and LMP.

Sieve Size (mm)	Filler Aggregate, Percentage Passing by Mass		
	WSA	LMP	Overval Range for Invidual Results [1]
2	100	100	100
0.125	89.6	94.0	85–100
0.063	81.5	80.8	70–100

Analysis of Table 1 indicates that both MPs comply with regulatory documents [1] in terms of their particle size distribution.

AT selected from the storage lake on the territory of the Lviv landfill for solid waste: Municipal Enterprise "Zbyranka" (Hrybovychi, Ukraine) was used as an activator of mineral powders. The approximate amount of acid tar in storage ponds is 300,000 tons. The initial moisture content of the selected acid tar was 47.4 wt.%, and the content of mechanical impurities was 3.6 wt.%. Therefore, a sample of acid tar was first prepared for further use. First, at a temperature of 105 °C, the sample was dried to a constant weight, followed by filtration at 105 °C to separate mechanical impurities. The characteristics of the prepared acid tar sample are given in Table 2.

Table 2. Main physical and chemical parameters of AT.

Index	Values	Procedure
Moisture (wt.%)	0.21	[35]
Ash (wt.%)	0.78	[36]
Density at 20 °C (kg/m^3)	982	[37]
Pour point (°C)	33	[38]
pH of water extract	1.9	–

As initial bitumen for stone mastic crude-oil-heavy pavement-oxidized bitumen of grade 70/100 from JSC "Ukrtatnafta", Ukraine was used. The operation characteristics of the taken bitumen are presented in Table 3. As per the tested indices, the present bitumen corresponds to grade 70/100 according to [39].

Table 3. Main physical and mechanical parameters of bitumen 70/100 (previously reported in [40]).

Index	Values	Procedure
Penetration at 25 °C, m·10^{-4} (dmm)	83	[41]
Softening point (°C)	50	[42]
Ductility at 25 °C (cm)	>100	[43]
Fraas breaking point (°C)	−18	[44]
Resistance to hardening at 163 °C: Retained penetration (%) Increase in softening poin (°C) Change of mass (absolute value; %)	- 74 8 0/4	[45]

Methods of testing bituminous binding materials are additionally described in [46].

Also, to produce SMA, used coarse aggregate of 4–8 mm and fine aggregate of 0–4 mm (granite quarry JSC "Polonskiy Gorniy Combinat", Khmelnytskyi region, Polonne, Ukraine) were used.

The stabilizing cellulose additive, Ukraine in the form of granules treated with bitumen in the amount of 15 wt.% was also used. Humidity of cellulose additive was 2 wt.%.

2.2. Experimental Procedure

2.2.1. Acid Tar Neutralization

Neutralization of AT was performed with 40% sodium hydroxide solution with stirring at a temperature of 80 °C to achieve a neutral reaction (pH = 7). During this, the neutralization reactions of organic sulfonic acids and sulfuric acid residues in the selected acid tar proceed according to the following reaction equations:

$$R—O—SO_2—OH + NaOH \rightarrow R—O—SO_2—ONa + H_2O \quad (1)$$

$$HO—SO_2—OH + 2NaOH \rightarrow NaO—SO_2—ONa + 2H_2O \quad (2)$$

After neutralization, the water was evaporated to a constant mass.

2.2.2. Chemical Activation of WSA and LMP

It is known that organic sulfonic acids and their salts, which are present in large quantities in AT, are good surfactants. Chemical activation was carried out by AT and NAT at an amount of 5 wt.% over the MP mass. AT and NAT were added to the MP according to the same scheme: the activator was added in the required amount, and then this mixture was homogenized in a ball mill at room temperature. The combination of grinding and activation operations yielded the application of activating composition at the moment of maximum chemical activity of a newly formed surface. After mixing the activator with the MP, this mixture was ground in a ball mill for 10 min using AT and 20 min using NAT. Since AT contains a large amount of a sulfonic acid, and the investigated mineral powders (WSA and LMP) contain alkaline components, we believe that chemical reactions (neutralization) take place during the activation process, that is, chemical activation occurs.

2.2.3. Designing SMA Composition

The composition of SMA was selected for type SMA 8 on unmodified bitumen 70/100 using non-activated and activated investigated MP. A universal composition was selected for SMA 8 (Table 4), which differed only in the MP variant used. The residual porosity for SMA 8 was in the range of 1.0–3.0 vol. %.

Table 4. Composition of SMA 8.

Name of Material	Content of Material in SMA (wt.%)
Coarse aggregate 4–8 mm	65
Fine aggregate 0–4 mm	20
Filler aggregate	15
Stabilizing additive	0.4
Bitumen 70/100	7.0

2.2.4. Testing of SMA

The study of SMA in the form of cylindrical samples (diameter and height: 71.4 mm; weight: 655.0 g) was carried out according to Ukrainian research methods since the used materials are local.

The average density of SMA was determined by hydrostatic weighing. Residual porosity was determined by the pores' volume in the SMA based on the given average density of the cylindrical samples and the actual density of the SMA mix. Water saturation was determined by the quantity of water, which is absorbed by a sample in the pre-set mode of saturation in a vacuum unit. The compression strength at 20 and 50 °C of SMA was determined on mechanical presses with a press-plate movement speed of (3.0 ± 0.1) mm/min. For testing, SMA samples were placed under the press plates with flat upper and lower faces of the cylinder. Before testing, samples were thermostat-conditioned in a vessel with water for (60 ± 5) min at the following temperatures: (50 ± 1) °C, (20 ± 1) °C. The samples for testing compression strength at 50 °C were placed (before thermostat-conditioning) into tight polyethylene bags to prevent their contact with water. Compression strength is a primary mechanical indicator and a water-saturation weather-resistant indicator that yields quick assessment of the effectiveness of the proposed solutions. The proposed studies were substantiated by many years of experience in their application in Ukraine.

2.2.5. X-ray Fluorescence Analysis (XRF)

XRF analysis of crushed stone was carried out by the Laboratory of Advanced Technologies for the Creation and Analysis of New Compounds and Functional Materials (Lviv Polytechnic National University, Lviv, Ukraine) using a spectrometer with the technical characteristics described in Table 5.

Table 5. Technical characteristics of an X-ray fluorescence analyzer (previously reported in [47]).

Spectrometer Units	Basic Specifications
Element detection range	from Na (atomic number Z = 11) to U (atomic number Z = 92) with helium blowdown or from K (atomic number Z = 19) to U (atomic number Z = 92) without helium use
X-ray tube (Rh78082)	Rh anode; 150 μm Be window; air-cooling
X-ray generator	voltage: 4–50 kV (±100 V); current: 0–100 μA (±0.2 μA); power: 5 W
Detector type	solid-state SDD with thermo-electrical cooling
Energy resolution	140 eV at 5.9 keV (^{55}Fe isotope)
Filters	Ti (400 μm); Al (800 μm); Ni (100 μm) (individual use); Ni (300 μm) with Al (300 μm) (in combination)
Software	ElvaX4.4 (Elvatech, Kyiv, Ukraine)
Quantitative analysis algorithms	fundamental parameters (for solid samples analysis based on their spectra); quadratic stepwise multiple regression (for liquid samples analysis, in general); manual spectra comparison (for alloys analysis)

The fluorescence spectrum of elements from Na to Cl was obtained using helium purging of the system to increase the detector resolution. In the case of elements with higher atomic numbers, helium purging was not necessary. The spectra interpretation (qualitative analysis) was carried out depending on the peaks' localization that matches the maximum energy of the electronic transition or by the presence of all maxima of each element's characteristic transitions. Quantitative analysis was conducted using the ElvaX4.4 program package by the algorithm of fundamental parameters deriving from the ratios of the peak areas of each element to the total peak area of all elements.

2.2.6. X-ray Diffraction (XRD) Analysis

Experimental arrays of the test samples' reflection intensities and angles were obtained on a desktop powder X-ray diffractometer (Malvern Panalytical, Malvern, United Kingdom) with the technical characteristics and in the 2θ-range described in Table 6. Preliminary processing of the experimental diffraction arrays in order to identify the phases was carried out using a Highscore + program package.

Table 6. Technical characteristics of the X-ray diffractometer.

Option	WSA	LMP
Start/final position of 2θ (°)	8.0074/89.9904	10.0109/84.9869
2θ step size (°)	0.0110	0.0220
2θ offset (°)	0.0000	
Divergence gap size (°)	0.4584	
Anode material	Cu	
Kα (Å)	1.54060	
Generator settings	15 mA, 40 kV	

2.2.7. Fourier-Transform Infrared Spectroscopy (FTIR)

The FTIR (Fourier-transform infrared spectroscopy, PerkinElmer, Llantrisant, UK) spectra samples were recorded on a Spectrum Two spectrometer using diamond U-ATR (The Universal Attenuated Total Reflectance Accessory, PerkinElmer, Llantrisant, UK) single-reflection accessory. The spectra (16 scans per spectrum) of the samples were collected in the mid-infrared wavenumber range of 4000 to 400 cm^{-1}, with a spectral resolution of 4 cm^{-1}.

2.2.8. Derivatography

The processes of WSA heat treatment were investigated using differential thermal analysis, which yielded monitoring of qualitative and quantitative changes in materials, the heating of which was accompanied by endo- or exothermic effects and mass change. The analysis was carried out on a modern device for thermal analysis, namely the Derivatograph OD-15,000, which yields, in addition to the differential temperature curve DTA and the mass change curve TG, the differential mass change curve DTG.

2.2.9. Determination of Hydrophobicity of MP and AMP

The tests were carried out in accordance with the Ukrainian standard [48]. The essence of the method is to determine the ability of AMP to not be wetted by water at room temperature. To do this, 500 mL of distilled water was poured into a chemical glass beaker. A weighted sample of up to 2 g was taken from the MP sample, which was poured on the water surface onto a chemical beaker with a spatula by lightly tapping it on the edge of the beaker. The beaker with distilled water and MP was left for 24 h for further examination. The powder was considered hydrophobic if, after 24 h, the entire particle mass of the weighted sample did not settle to the bottom of the beaker and the MP was not wetted with water.

3. Results and Discussion

To obtain the so-called activated mineral powders, which are used in the production of SMA, industrial waste was used, namely paper (WSA and oil refining) AT. This solves two problems: the first is ecological since these wastes (especially AT) pollute the environment during their open storage; and the second problem is the shortage of quality materials for road construction. In other words, this work is dedicated to the creation of a comprehensive approach for the gradual and effective disposal of harmful acid tar dumps and paper production waste in order to obtain new ecological road-construction materials. The study of these components was carried out at the first stage.

3.1. Properties of WSA and LMP, as a Filler Aggregate for SMA

First, elemental WSA and LMP were determined using XRF analysis (Figures 2 and 3, Table 7). LMP was studied in parallel with WSA because it is a traditional mineral powder.

The obtained results (Table 7) show that WSA has a lower content of Ca and higher contents of Si and Al compared to traditional LMP, indicating the presence of sand (SiO_2) and alumina (Al_2O_3) in WSA. Therefore, it is necessary to study the mineralogical composition of WSA.

It is known that the mineralogical composition of the obtained WSA significantly depends on the technology and conditions of PS firing. Then, the mineralogical composition of PS (Figure 4, Table 8) and WSA (Figure 5, Table 9) was determined using XRD analysis.

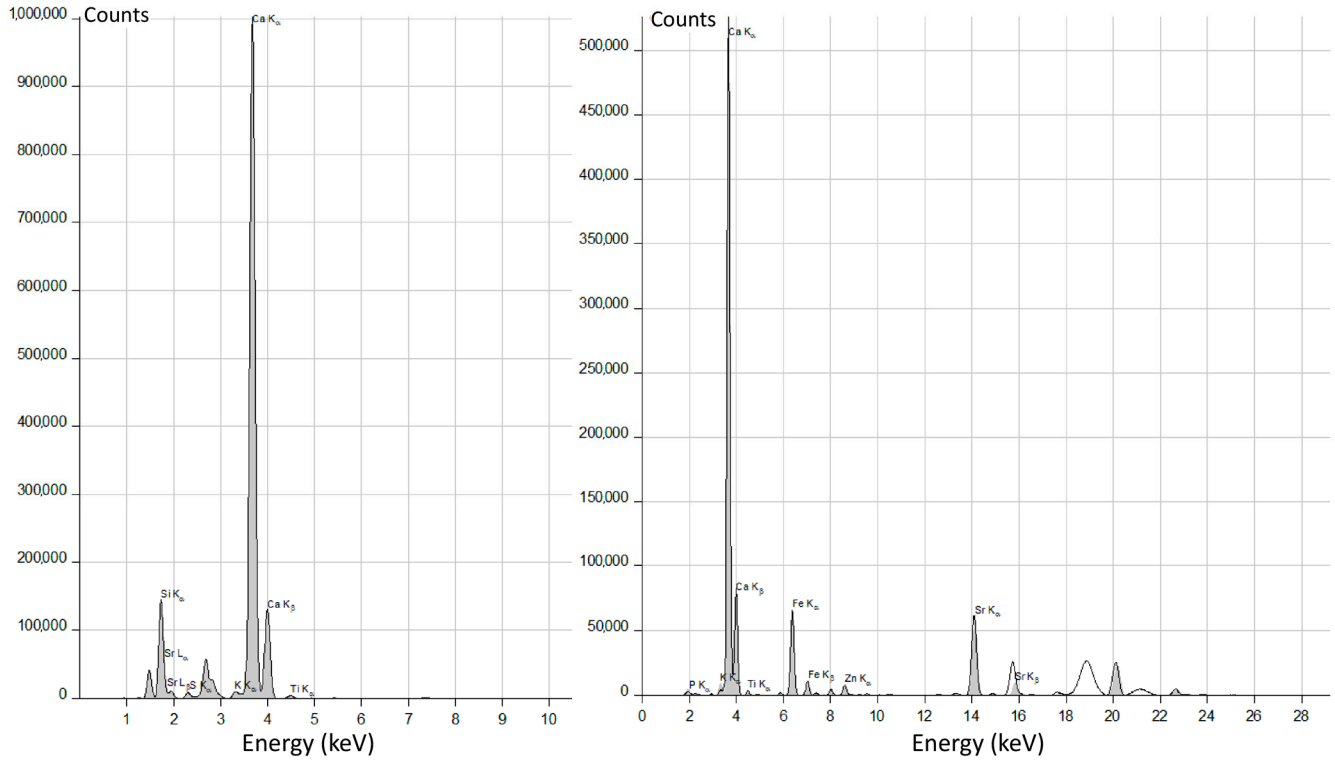

Figure 2. XRF analysis of WSA.

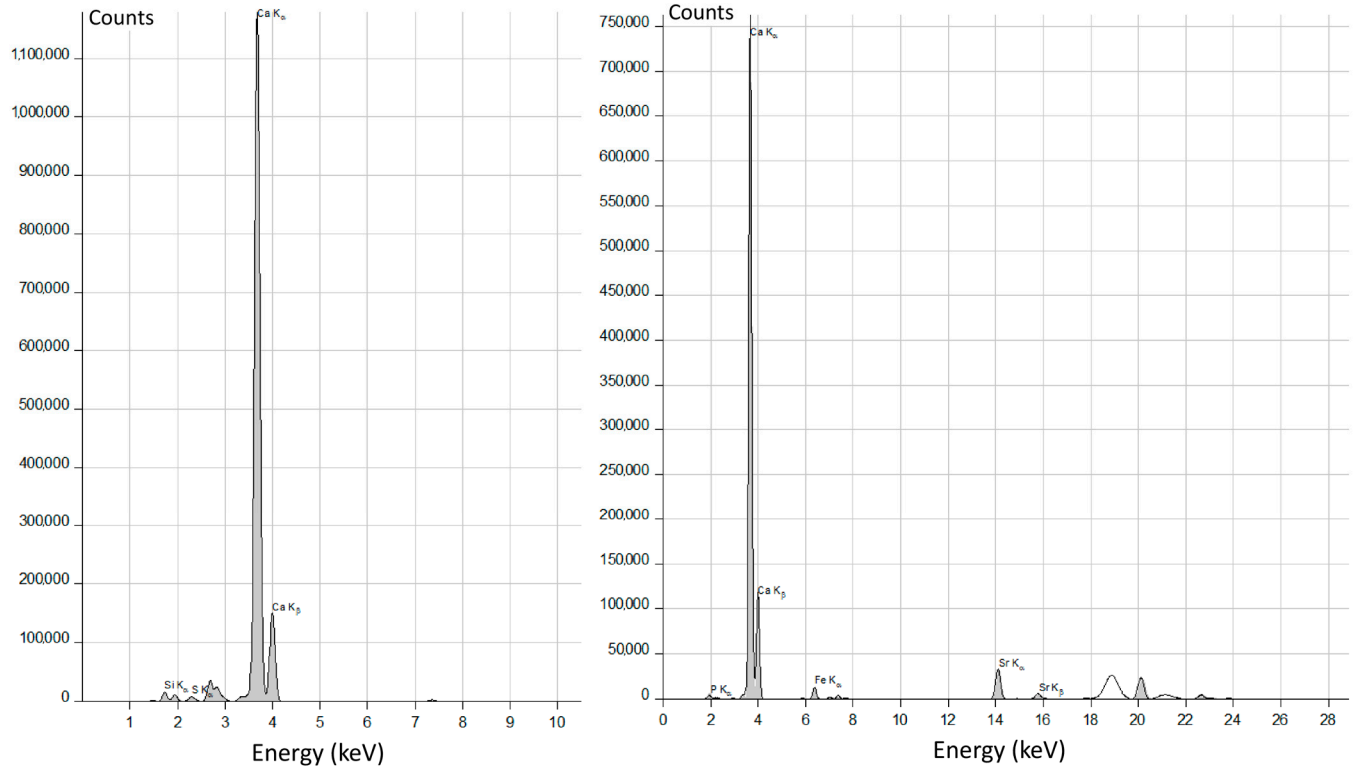

Figure 3. XRF analysis of LMP.

Table 7. The elemental composition of WSA and LMP was determined by XRF analysis.

Element	Peak Intensity (arb.un.)		Content (wt.%)	
	WSA	LMP	WSA	LMP
Ca	2,645,565	3,828,135	42.82 ± 0.03	68.22 ± 0.02
Si	1,087,852	114,304	11.01 ± 0.02	1.37 ± 0.01
Al	304,497	9724	6.88 ± 0.03	0.31 ± 0.02
* Fe	376,972	74,391	0.94 ± 0.00	0.37 ± 0.00
* K	40,701	–	0.83 ± 0.02	–
* Ti	18,312	–	0.29 ± 0.01	–
S	67,797	63,461	0.11 ± 0.00	0.10 ± 0.00
P	28,098	20,093	0.10 ± 0.00	0.07 ± 0.00
Sr	488,861	257,014	0.09 ± 0.00	0.09 ± 0.00

* Isomorphic impurities of kaolinite.

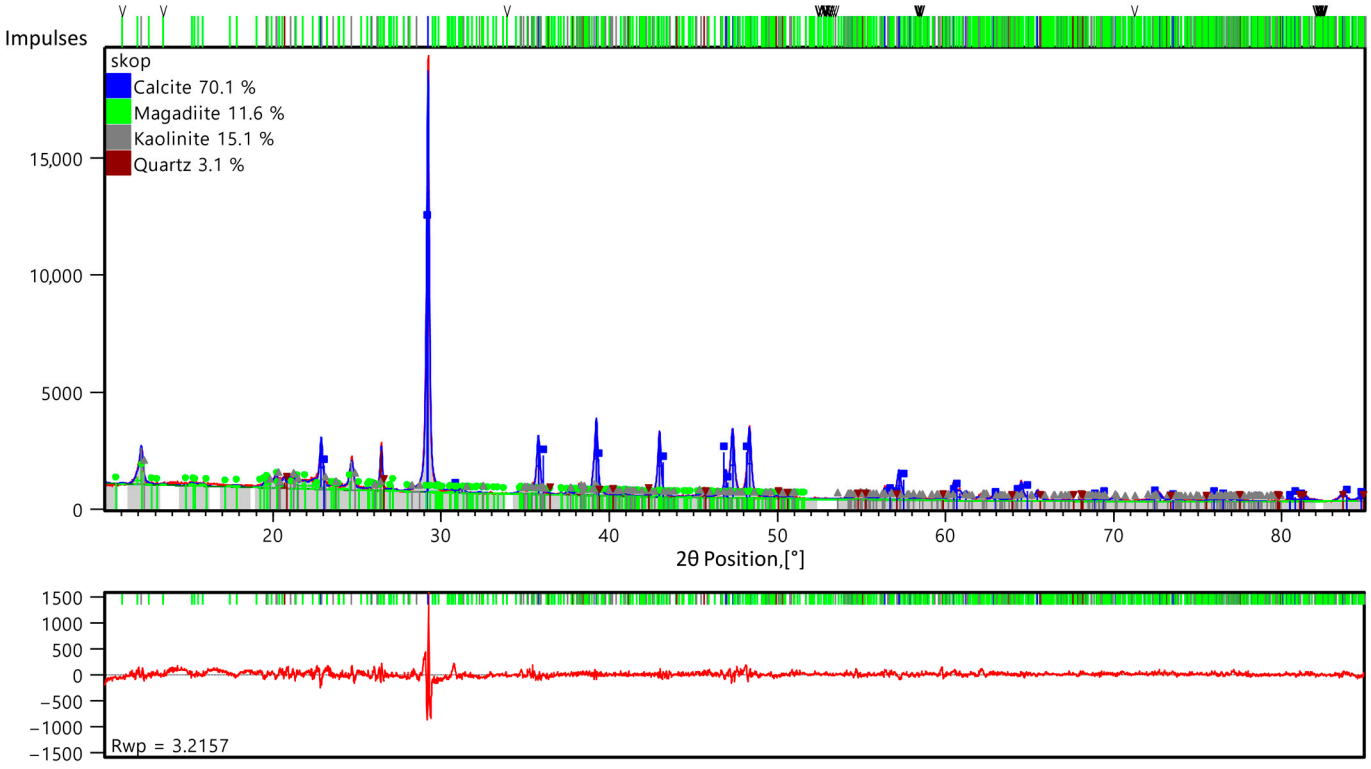

Figure 4. Results of XRD patterns refinement of PS by Highscore + program package (Rwp = 3.2157).

Table 8. Mineralogical composition of PS determined using XRD.

Name	Chemical Formula	Content (wt.%)
Calcite	$6CaCO_3$ ($Ca_6C_6O_{18}$)	70.1
Magadiite	$Si_{24}O_{52}$	11.6
Kaolinite	$Al_2O_3 \cdot 2SiO_2$ ($Al_2Si_2O_9$)	15.1
Quartz	Si_6O_6	3.1

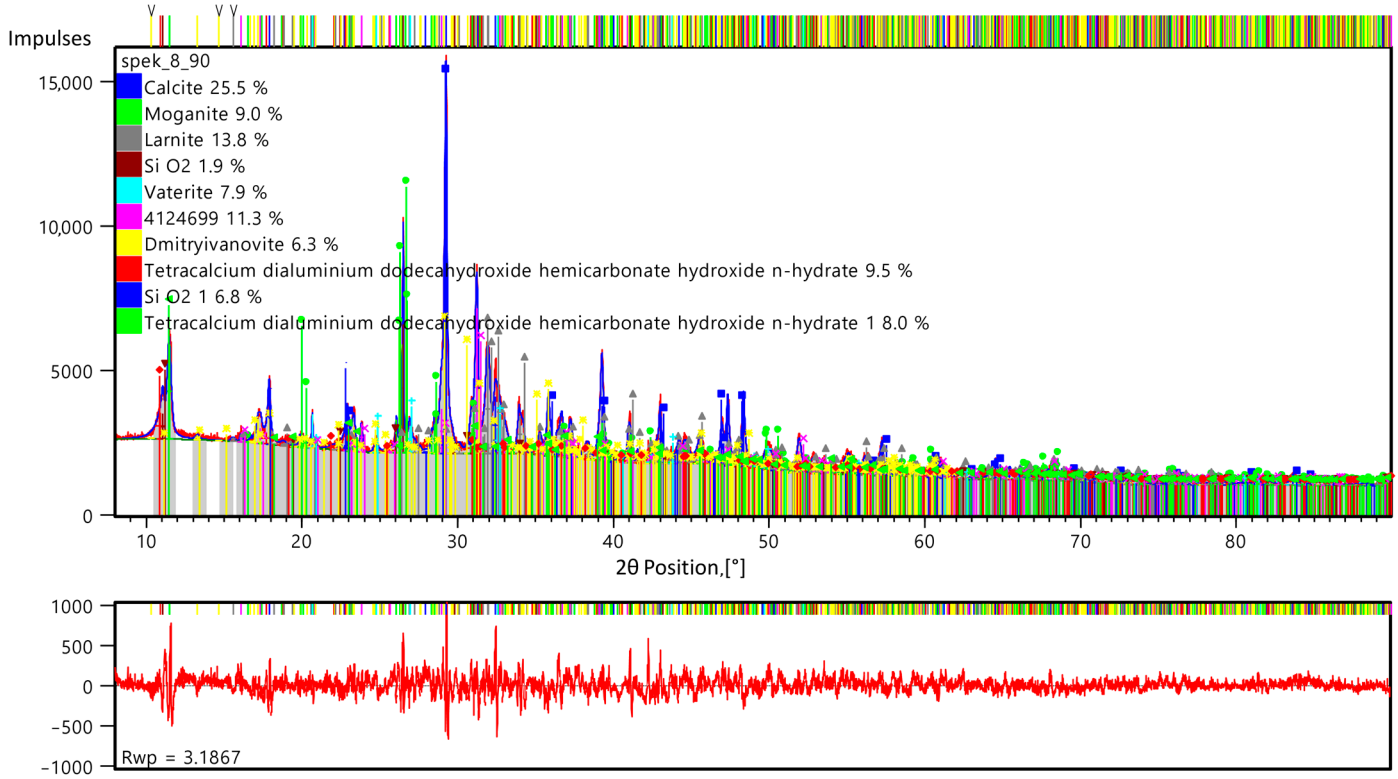

Figure 5. Results of XRD patterns' refinement of WSA by Highscore+ program package (Rwp = 3.1867).

Table 9. Mineralogical composition of WSA determined using XRD.

Name	Chemical Formula	Content (wt.%)
Calcite	$6CaCO_3$ ($Ca_6C_6O_{18}$)	25.5
Moganite	$12SiO_2$ ($Si_{12}O_{24}$)	9.0
Larnite	$8CaO{\cdot}4SiO_2$ ($Ca_8Si_4O_{16}$)	13.8
SiO_2	$18SiO_2$ ($Si_{18}O_{36}$)	1.9
Vaterite	$2CaCO_3$ ($Ca_2C_2O_6$)	7.9
–	$4CaO{\cdot}2Al_2O_3{\cdot}2SiO_2$ ($Ca_4Al_4Si_2O_{14}$)	11.3
Dmitryivanovite	$8CaO{\cdot}8Al_2O_3$ ($Ca_8Al_{16}O_{32}$)	6.3
Tetracalcium dialuminium dodecahydroxide hemicarbonate hydroxide n-hydrate	$Al_6Ca_{12}O_{55.5}C_{1.5}$	9.5
SiO_2	$8SiO_2$ (Si_8O_{16})	6.8
Tetracalcium dialuminium dodecahydroxide hemicarbonate hydroxide n-hydrate	$Ca_{12}Al_6O_{55.2}C_{2.4}$	8.0

Table 8 shows that PS mainly consists of calcite (70.1 wt.%). Calcite undergoes thermal and thermochemical dissociation during firing. Calcite transformation as a result of firing is confirmed by its decrease from 70.1 wt.% (Table 8) to 25.5 wt.% (Table 9).

The theoretical temperature of thermal dissociation of $CaCO_3$ is 910 °C:

$$CaCO_3 \rightarrow CaO + CO_2 \quad (3)$$

Thermochemical dissociation of $CaCO_3$ begins in the presence of reactive active phases in PS, particularly kaolinite (15.1 wt.%; Table 8), already at a temperature of 600–700 °C, according to the following scheme:

$$CaCO_3 + Al_2O_3 \cdot 2SiO_2 \rightarrow mCaO \cdot SiO_2 + nCaO \cdot Al_2O_3 \quad (4)$$

The passage of this reaction indicates the presence of Larnite (13.8 wt.%) and Dmitryivanovite (6.3 wt.%) phases in WSA (Table 9). This process is the beginning of solid phase interactions, due to which the phase composition of WSA is formed.

Figure 6 shows the PS derivative diagram, which characterizes the processes occurring in the solid-fuel heat generator during the burning of PS briquettes.

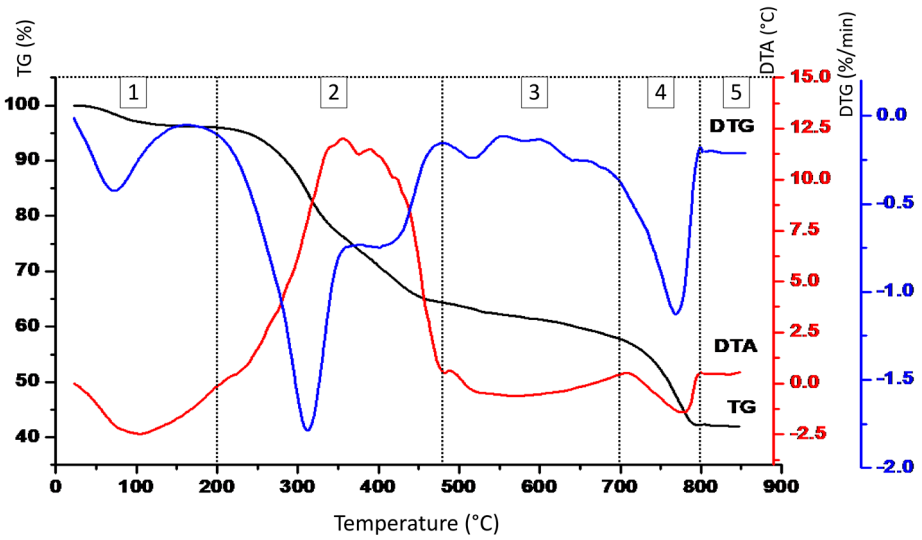

Figure 6. Derivatogram of PS: TG—mass change curve of the sample; DTA—differential temperature curve illustrating the release or absorption of heat by a sample; DTG—differential mass change curve of the sample (rate of mass change).

PS briquettes that burn in the combustion chamber have an even higher temperature in their core, which promotes sintering and its subsequent slag under the influence of combustion products and carbon dioxide from $CaCO_3$ decarburization.

The derivative diagram illustrates the dynamics and phase transformations of PS combustion. At the intersection points of the DTA curve with its "zero" line, five characteristic zones are distinguished (Figure 6):

(1) evaporation of moisture and physically bound H_2O (0–200 °C);
(2) combustion of volatiles (200–480 °C);
(3) coke burning and calcite interaction with kaolinite (480–700 °C);
(4) calcite decarburization (700–800 °C);
(5) formation of Ca silicates and Ca aluminates (>800 °C), which proves their high content in WSA (Table 9).

The humidity of PS was W = 4% (according to the projections of the TG curve points in the first zone) and the yield of volatile substances was 96 − 64 = 32% (according to the TG projection in the second zone).

Comparing Tables 8 and 9, the mineralogical composition of WSA is much more complex compared to PS and depends on many factors.

Also, for comparison, the mineralogical composition of traditional LMP (Figure 7; Table 10), which is used to obtain different types of SMA, was determined using XRD analysis.

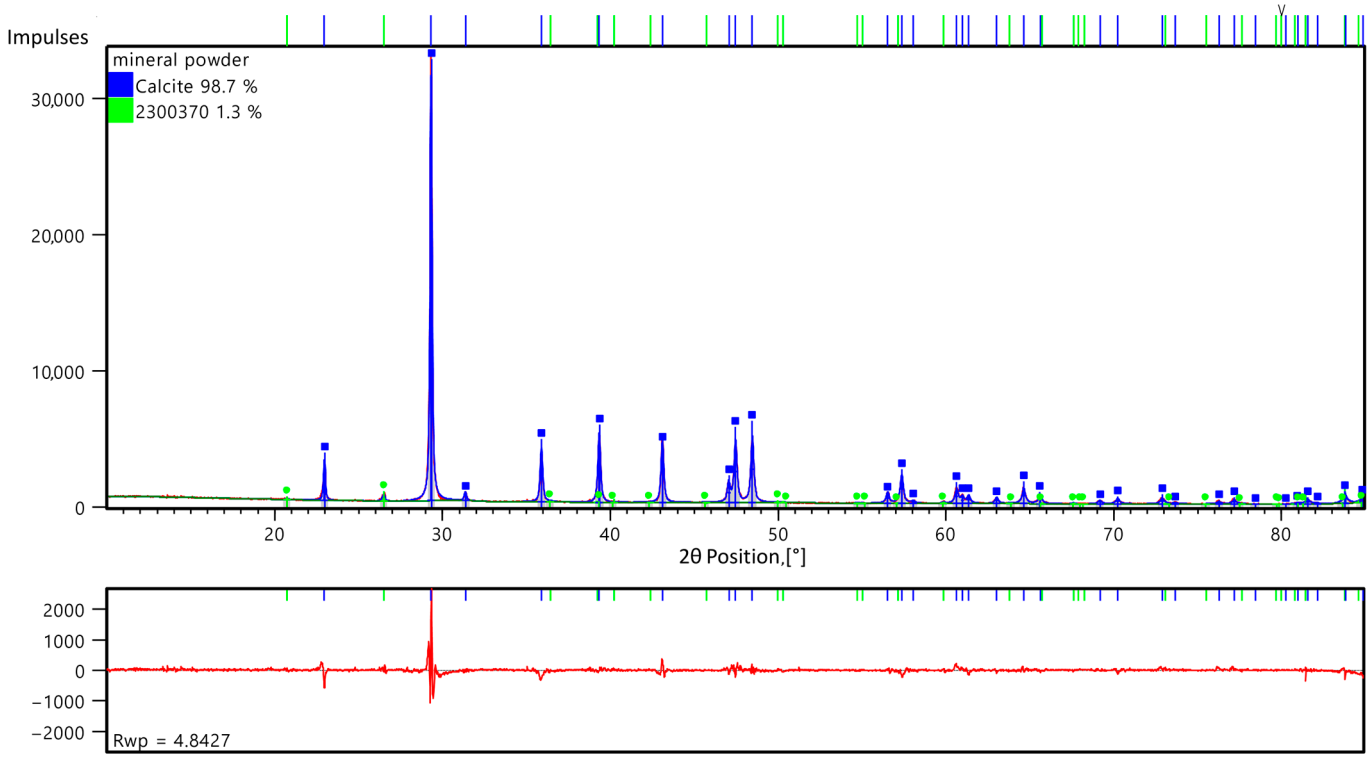

Figure 7. Results of XRD patterns refinement of LMP by Highscore + program package (Rwp = 4.8427).

Table 10. Mineralogical composition of LMP determined using XRD.

Name	Chemical Formula	Content (wt.%)
Calcite	$6CaCO_3$ ($Ca_6C_6O_{18}$)	99.1
SiO_2	$3SiO_2$ (Si_3O_6)	0.9

Commercial LMP belongs to the highest category in terms of calcium carbonate content according to [1], namely CC_{90}, as it contains more than 90 wt. % calcium carbonate (99 wt.%; Table 10). PS is more similar in mineralogical composition to traditional LMP than WSA, but has significant disadvantages:

(1) high humidity;
(2) high flammability due to the presence of volatile substances (already ignites at 80–100 °C);
(3) impossibility of achieving the required granulometric composition (≤0.063 mm).

Therefore, fired PS, i.e., WSA, which is devoid of all these disadvantages, was used as a traditional substitute for MR in the production of SMA.

3.2. Activator for LMP and WSA

As LMP and WSA activators, other wastes were used, already from oil refineries, such as AT. The expediency of neutralizing BP and obtaining NAT was also studied. To study the chemical structure of these activators, FTIR spectra were recorded for AT and NAT (Figure 8).

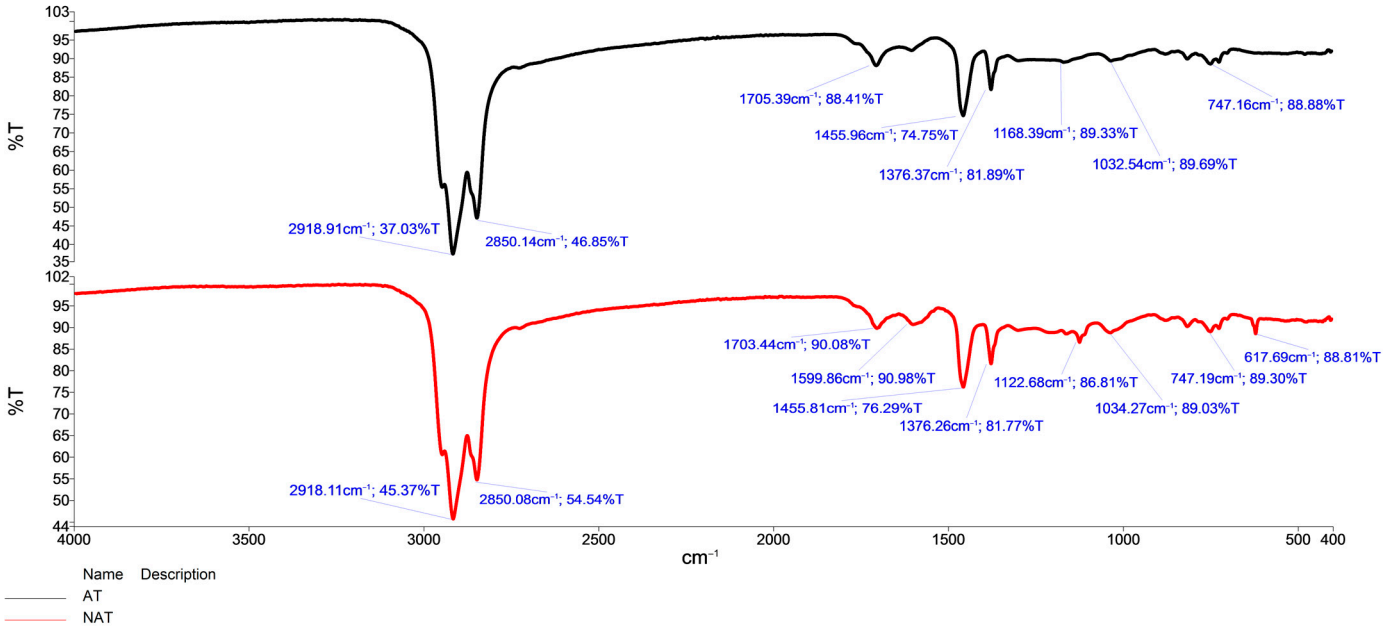

Figure 8. FTIR spectrum of AT and NAT.

AT and NAT consist of three main components:

(1) hydrocarbons (R–H);
(2) interaction products of Hydrocarbons with sulfuric acid (R–O–SO_2–R'; R–O–SO_2–O–R');
(3) acids (R–O–SO_2–OH; H_2SO_4) in the case of AT and salts (R–O–SO_2–ONa; Na_2SO_4) in the case of NAT.

The interpretation of the main absorption bands of the FTIR spectra of AT and NAT is given in Table 11.

Table 11. The main peaks of the FTIR spectra of AT and NAT [49].

Groups	AT		NAT	
	cm^{-1}	**% T**	**cm^{-1}**	**% T**
Arenes	1705.39	88.41	1703.44	90.08
	1604.00	92.55	1599.86	90.98
Disubstituted arenes	747.16	88.88	747.19	89.30
CH_2 group (symmetric valence vibrations)	2850.14	46.85	2850.08	54.54
CH_3 group (asymmetric valence vibrations)	2918.91	37.03	2918.11	45.37
SO_2 group in R–O–SO_2–R' (asymmetric valence vibrations)	1455.81	74.55	1455.81	76.29
Covalent bonding group in R–O–SO_2–O–R'	1376.37	81.89	1376.26	81.77
SO_2 group in NAT (asymmetric valence vibrations), which corresponds to SO_4^{-2}	–	–	1122.68	86.81
SO_2 group	1032.54	89.69	1034.27	89.03
R–SO_2–ONa	–	–	617.69	88.81

3.3. Activated Filler Aggregate

LMP and WSA were activated by AT and NAT in a ball mill. After that, the analysis of the obtained AMP was carried out—the wettability index was determined as shown in Figures 9 and 10.

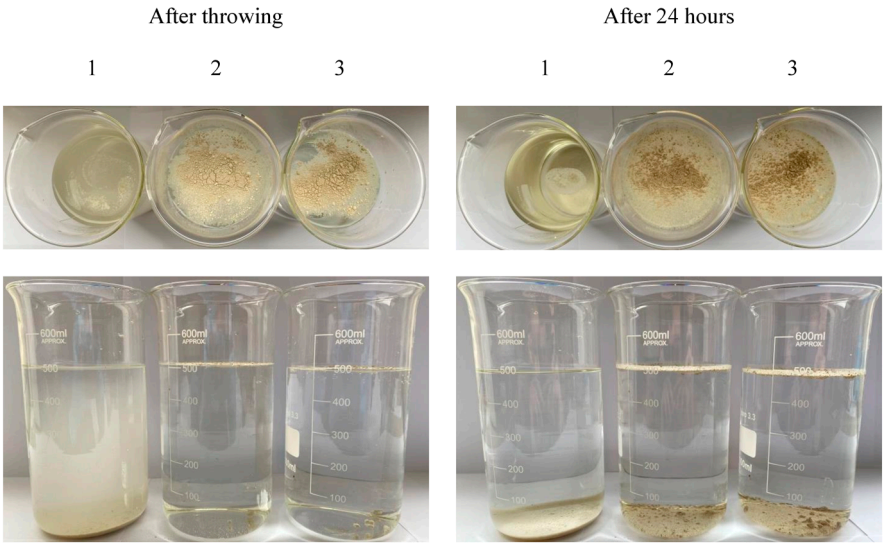

Figure 9. Wettability: 1—LMP (hydrophilic); 2—LMP + AT (hydrophobic); 3—LMP + NAT (hydrophobic).

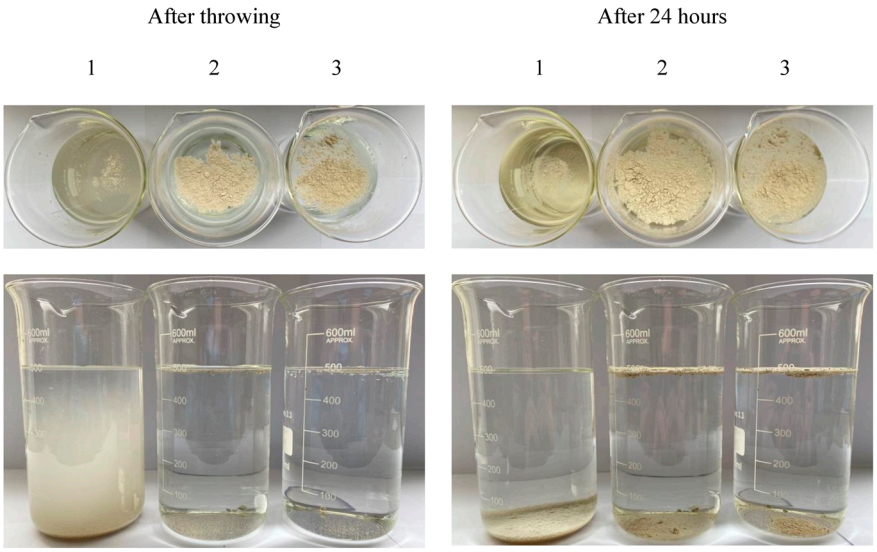

Figure 10. Wettability: 1—WSA (hydrophilic); 2—WSA + AT (hydrophobic); 3—WSA + NAT (hydrophobic).

Figures 9 and 10 show that deactivated LMP and WSA are hydrophilic, that is, they were well wetted by water. All obtained AMP samples were hydrophobic, that is, they were poorly wetted by water, which is the main requirement for AMP.

AMP application in road construction makes it possible to significantly increase the resistance of such roads to the effects of moisture and frost, and as a result, reduce the occurrence of cracks and increase the service life of such a coating.

Figure 11 shows possible chemical transformations in SMA using MP activated by AT.

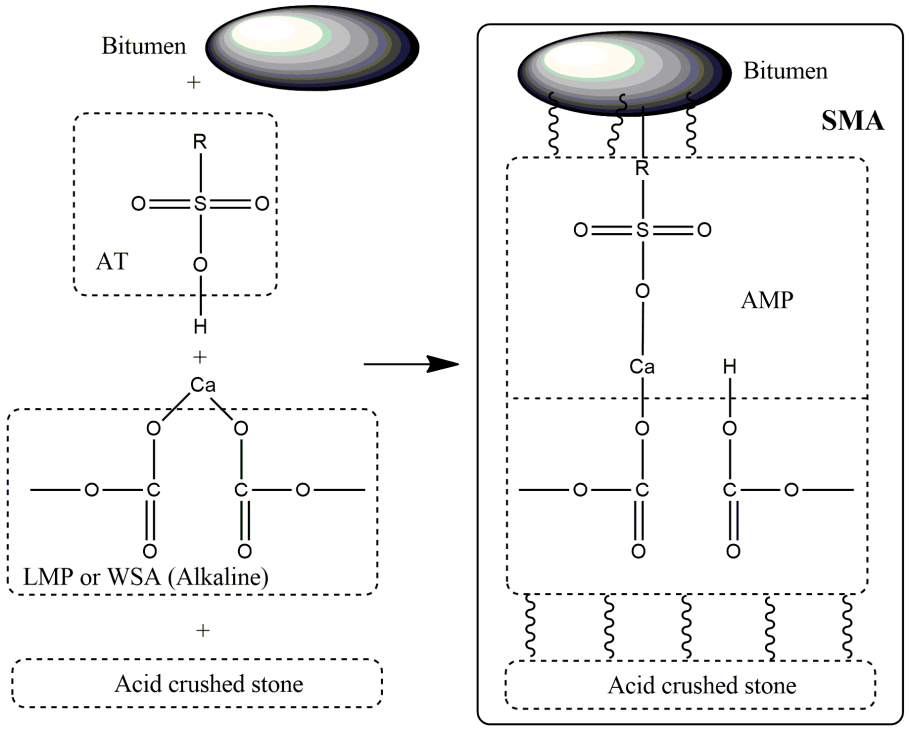

Figure 11. Possible chemical transformations in SMA using MP activated AT.

AT can be neutralized directly in MP (LMP or WSA), while a strong bond between AT and MP is formed, that is, chemical activation takes place. The presence of acids (R–O–SO_2–OH; H_2SO_4) in AT was confirmed by FTIR spectroscopy (Table 11), and the presence of alkaline components in LMP and WSA was confirmed by XRD analysis (Tables 9 and 10, respectively). For example, the following chemical reactions are possible between acids and calcite during AT activation:

$$2R—O—SO_2—OH + CaCO_3 \rightarrow (R—O—SO_2—O)_2Ca + H_2O + CO_2 \quad (5)$$

$$H_2SO_4 + CaCO_3 \rightarrow CaSO_4 + H_2O + CO_2 \quad (6)$$

This interaction does not occur with NAT as an activator.

In our opinion, the formed AMPs do not pose a significant threat to the environment since the content of the AT activator in AMPs is insignificant (5 wt. % over MP mass) and chemical neutralization of sulfonic acids contained in AT is also possible. However, it is advisable to investigate the aspects related to environmental impact, which will be studied in further research.

3.4. Stone Mastic Asphalt

To determine the influence of WSA and LMP on the physical and mechanical properties of SMA, six compositions of SMA 8 were selected (Table 12).

The analysis of Table 12 indicates that WSA can completely replace traditional LMP since the main physical and mechanical properties of SMA 8 using WSA are practically the same as using traditional LMP. However, the content of the pure phase of calcite in WSA (25.5 wt.%) (Table 9) and LMP (99.1 wt.%) (Table 11) differs significantly. In other words, the low content of calcium carbonate in WSA does not lead to a negative impact on the main physical and mechanical parameters of the obtained SMA 8.

During the activation of LMP and WSA (Table 12), AT decreases water saturation, and in the case of WSA, this decrease is much greater (from 2.3 to 1.1 vol %), which indicates the high hydrophobicity of AMP (Figure 10) and the undergoing chemical activation (Table 12). Compression strength at 20 °C also increases slightly with the activation of AT.

The use of NAT for the activation of LMP and WSA is impractical, as all the investigated physical and mechanical properties of SMA 8 deteriorate, due to the impossibility of chemical activation (NAT + LMP or WSA).

Table 12. Physico-mechanical properties of SMA 8.

No.	Composition of SMA 8	Average Density (g/cm^3)	Water Saturation (vol. %)	Compression Strength at (MPa)	
				20 °C	50 °C
Filler Aggregate					
1	LMP	2.33	1.8	5.1	1.1
2	WSA	2.33	2.3	5.2	1.2
Activated filler aggregate					
3	LMP + AT	2.33	1.5	5.4	1.1
4	LMP + NAT	2.32	2.0	4.1	0.9
5	WSA + AT	2.33	1.1	5.3	1.2
6	WSA + NAT	2.32	2.1	3.2	0.9
Requirements to SMA-8 according to the standard [50]		-	Not more than 3.0	Not less than	
				3.2	0.9

4. Conclusions

The current study was conducted by means of the application of oil refining (acid tar) and paper (wastepaper sludge ash) waste to obtain new road materials. Therefore, two problems are solved: the first is ecological, and the second is a shortage of building materials.

First, the study of these materials was carried out using X-ray diffraction analysis, and the mineralogical composition of wastepaper sludge ash was established; compared to the composition of traditional limestone mineral powder, it is much more complex. In addition to the calcite phase, it also contains other phases in significant quantities. Using FTIR spectroscopy, the presence of free sulfuric acid and organic sulfonic acids was established in acid tar.

The chemical activation process of wastepaper sludge ash and limestone mineral powder with original and neutralized acid tar was carried out in a ball mill. According to the Ukrainian method, it was established that the inactivated wastepaper sludge ash and limestone mineral powder are hydrophilic, that is, well wetted with water, and the obtained activated samples are hydrophobic, i.e., poorly wetted with water, which is the main requirement for the production of activated mineral powder.

The obtained results show that wastepaper sludge ash can completely replace traditional limestone mineral powder since the main physical and mechanical parameters of stone mastic asphalt (SMA 8) with their use are practically the same.

The activation efficiency of the initial acid tar of wastepaper sludge ash and limestone mineral powder has been proven, allowing for SMA 8 to increase water resistance, and in the case of wastepaper sludge ash, this reduction is much greater (from 2.3 to 1.1 vol %), which indicates it is highly hydrophobic. The use of neutralized acid tar for activation is not advisable, because there is a deterioration of all the investigated physical and mechanical properties of SMA 8.

The strength characteristics of stone mastic asphalt SMA 8 with activated filler aggregate (using AT) increase slightly by 0.1–0.3 MPa, but water saturation decreases by 17–52%.

The obtained research results are valid for other types of asphalt concrete with high probability.

Author Contributions: Conceptualization, V.G., I.S. and M.B.; methodology, I.S. and V.H.; software, Y.D. and N.V.; validation, M.B., V.G. and K.S.; formal analysis, I.S., P.S. and V.G.; investigation, V.H., I.S. and V.S.; resources, Y.D. and N.V.; data curation, I.S., V.G. and V.H.; writing—original draft preparation, V.G. and I.S.; writing—review and editing, M.B., K.S. and P.S.; visualization, V.G.; supervision, M.B.; project administration, Y.D. and V.G. All authors have read and agreed to the published version of the manuscript.

Funding: This work was supported by the National Research Foundation of Ukraine, Kyiv (Grant No. 2020.02/0038).

Institutional Review Board Statement: Not applicable.

Informed Consent Statement: Not applicable.

Data Availability Statement: Data supporting reported results are stored by V. Gunka.

Acknowledgments: All authors thank the Laboratory of Advanced Technologies, Creation and Physico-Chemical Analysis of a New Substances and Functional Materials for providing XRD and XRF analysis.

Conflicts of Interest: The authors declare no conflict of interest.

Abbreviations

AMP	activated mineral powder
AT	initial acid tar
HMA	hot asphalt concrete
LMP	limestone mineral powder
NAT	neutralized acid tar
SMA	stone mastic asphalt
WSA	wastepaper sludge ash
XRD	X-ray diffraction
XRF	X-ray fluorescence
MP	mineral powder
PS	paper sludge

References

1. *EN 13043*; Aggregates for Bituminous Mixtures and Surface Treatments for Roads, Airfields and Other Trafficked Areas. European Committee for Standardization (CEN): Brussels, Belgium, 2002.
2. *EN 13108-1*; Bituminous Mixtures. Material Specifications. Asphalt Concrete. European Committee for Standardization (CEN): Brussels, Belgium, 2016.
3. *EN 13108-5*; Bituminous Mixtures. Material Specifications. Stone Mastic Asphalt. European Committee for Standardization (CEN): Brussels, Belgium, 2016.
4. Tiwari, N.; Baldo, N.; Satyam, N.; Miani, M. Mechanical Characterization of Industrial Waste Materials as Mineral Fillers in Asphalt Mixes: Integrated Experimental and Machine Learning Analysis. *Sustainability* **2022**, *14*, 5946. [CrossRef]
5. Gunka, V.; Sidun, I.; Solodkyy, S.; Vytrykush, N. Hot asphalt concrete with application of formaldehyde modified bitumen. In *International Conference Current Issues of Civil and Environmental Engineering Lviv-Košice–Rzeszów*; Springer: Cham, Switzerland, 2019; pp. 111–118. [CrossRef]
6. Gunka, V.; Demchuk, Y.; Sidun, I.; Miroshnichenko, D.; Nyakuma, B.B.; Pyshyev, S. Application of phenol-cresol-formaldehyde resin as an adhesion promoter for bitumen and asphalt concrete. *Road Mater. Pavement Des.* **2021**, *22*, 2906–2918. [CrossRef]
7. Remisova, E.; Decky, M.; Kovac, M. The influence of the asphalt mixture composition on the pavement surface texture and noise emissions production. In Proceedings of the 14th International Multidisciplinary Scientific Conference SGEM, Albena, Bulgaria, 17–26 June 2014; pp. 583–590.
8. Lima, M.S.S.; Thives, L.P.; Haritonovs, V.; Gschösser, F. The Influence of Alternative Fillers on the Adhesive Properties of Mastics Fabricated with Red Mud. *Materials* **2020**, *13*, 484. [CrossRef] [PubMed]
9. Diab, A.; Enieb, M. Investigating influence of mineral filler at asphalt mixture and mastic scales. *Int. J. Pavement Res. Technol.* **2018**, *11*, 213–224. [CrossRef]
10. Krayushkina, K.; Akmaldinova, O.; Fedorenko, K.; Skrypchenko, O. The Use of Mineral Powders of Various Nature to form the Structure of Asphalt Concrete. In Proceedings of the 13th International Conference TRANSBALTICA, Vilnius, Lithuania, 15–16 September 2022; pp. 175–188. [CrossRef]

11. Tian, P.; Peng, K.; Dong, H.; Li, Y.; Dong, W. The Effect of Mineral Powder on the Surface/Interface of Aggregates and Asphalt. *Ann. De Chim.-Sci. Des Matériaux* **2021**, *45*, 281–290. [CrossRef]
12. Choi, M.J.; Kim, Y.J.; Kim, H.J.; Lee, J.J. Performance evaluation of the use of tire-derived fuel fly ash as mineral filler in hot mix asphalt concrete. *J. Traffic Transp. Eng. (Engl. Ed.)* **2020**, *7*, 249–258. [CrossRef]
13. Hamedi, G.H.; Sohrabi, M.; Sakanlou, F.; Tahami, S.A. Investigating the Effect of Various Fillers on Cohesive Failure Mechanism in Asphalt Mixtures. *Period. Polytech. Civ. Eng.* **2020**, *64*, 144–155. [CrossRef]
14. Liu, Z.; Wang, Y. Laboratory research on asphalt mastic modified with activated carbon powder: Rheology, micro-structure, and adhesion. *Road Mater. Pavement Des.* **2021**, *22*, 1424–1441. [CrossRef]
15. Akter, R.; Hossain, M.K.; Anwar, M.S.; Rahman, K. Performance evaluation of coal dust and wood powder ash as alternates of conventional filler in the asphalt concrete. *Sustain. Eng. Innov.* **2022**, *4*, 82. [CrossRef]
16. Naveed, H.; ur Rehman, Z.; Khan, A.H.; Qamar, S.; Akhtar, M.N. Effect of mineral fillers on the performance, rheological and dynamic viscosity measurements of asphalt mastic. *Constr. Build. Mater.* **2019**, *222*, 390–399. [CrossRef]
17. Pasandín, A.R.; Pérez, I. The influence of the mineral filler on the adhesion between aggregates and bitumen. *Int. J. Adhes. Adhes.* **2015**, *58*, 53–58. [CrossRef]
18. Ruíz-Ibarra, J.F.; Rondón-Quintana, H.A.; Chaves-Pabón, S.B. Behavior of a warm mix asphalt containing a blast furnace slag. *Int. J. Civ. Eng.* **2020**, *18*, 325–334. [CrossRef]
19. Tahami, S.A.; Arabani, M.; Mirhosseini, A.F. Usage of two biomass ashes as filler in hot mix asphalt. *Constr. Build. Mater.* **2018**, *170*, 547–556. [CrossRef]
20. Wu, B.; Liu, L.; Feng, Y. Evaluation of steel slag powder as filler in hot-mix asphalt mixtures. *Adv. Civ. Eng. Mater.* **2018**, *7*, 64–72. [CrossRef]
21. Hidei, V.; Sidun Iu Hunyak, O.; Stanchak, S.; Bidos, V. Application of wastepaper sludge ash as mineral powder for hot asphalt concrete mix. *Theory Build. Pract.* **2020**, *2*, 42–47. [CrossRef]
22. Sobol, K.; Solodkyy, S.; Petrovska, N.; Belov, S.; Hunyak, O.; Hidei, V. Chemical Composition and Hydraulic Properties of Incinerated Wastepaper Sludge. *Chem. Chem. Technol.* **2020**, *14*, 538–544. [CrossRef]
23. Solodkyy, S.; Hidei, V.; Sidun, I.; Turba, Y. Using waste paper sludge ash (wsa) as a material for soil strengthening for the construction of layers of roadwear. *Theory Build. Pract.* **2021**, *3*, 85–91. [CrossRef]
24. Kwetkus, B.A. Particle triboelectrification and its use in the electrostatic separation process. *Part. Sci. Technol.* **1998**, *16*, 55–68. [CrossRef]
25. Trautvain, A.; Yadykina, V.; Gridchin, A.; Pashkova, C. Evaluating the effectiveness of producing the activated mineral powders from technogenic raw materials for asphalt mixtures. *Procedia Eng.* **2015**, *117*, 350–356. [CrossRef]
26. Barisoglu, E.N.; Oliveira Costa, J.; Theys, F.; Blom, J.; Vuye, C.; Van den bergh, W. The effect of active filler type, compaction method and slag-based geopolymer on volumetric and mechanical properties of cold foamed bitumen mixes with 100% RAP. *Road Mater. Pavement Des.* **2023**, 1–18. [CrossRef]
27. Solodkyy, S.Y.; Ilnytskyi, Z.M.; Poliuzhyn, I.P.; Tsiupko, F.I. Application Features for the Activator of Mineral Materials "RENA-Aquador" for Asphalt Concrete Pavings. In *International Conference Current Issues of Civil and Environmental Engineering Lviv-Košice–Rzeszów*; Springer: Cham, Switzerland, 2019; pp. 480–487. [CrossRef]
28. Yue, P.C.; Liu, P.F.; Dong, J.Z.; Ding, P.P. Research of Road Application Performances of Asphalt Mixtures with Active Mineral Powder. In *Key Engineering Materials*; Trans Tech Publications Ltd.: Stafa-Zurich, Switzerland, 2014; Volume 599, pp. 218–223. [CrossRef]
29. Hadadi, V.; Moradi, A. A novel method for refining of acidic sludge and mixing with vacuum bottom to improve bitumen properties. *Pet. Sci. Technol.* **2019**, *37*, 1529–1538. [CrossRef]
30. Fakhri, M.; Arzjani, D.; Ayar, P.; Mottaghi, M.; Arzjani, N. Performance Evaluation of WMA Containing Re-Refined Acidic Sludge and Amorphous Poly Alpha Olefin (APAO). *Sustainability* **2021**, *13*, 3315. [CrossRef]
31. Khlibyshyn, Y.; Pochapska, I.Y.; Grynyshyn, O.B.; Gnativ, Z.Y. The study of the fabrication of bitumen from acid tars and oil residues. *Issues Chem. Chem. Technol.* **2018**, *5*, 161–167.
32. Khlibyshyn, Y.; Pochapska, I.; Grynyshyn, O.; Hladkyi, O. Preparation of bitumen using acidic tars. In Proceedings of the 2nd International Scientific Conference «Chemical Technology and Engineering», Lviv, Ukraine, 24–28 June 2019; p. 394. [CrossRef]
33. Frolov, A.F.; Aminov, A.N.; Timrot, S.D. Composition and properties of acid tar and asphalt produced from acid tar. *Chem. Technol. Fuels Oils (Engl. Transl.)* **1982**, *17*, 284–288. [CrossRef]
34. Zmamou, H.; Leblanc, N.; Levacher, D.; Kubiak, J. Recycling of high quantities of wastepaper sludge ash for production of blended cements and alternative materials. *Environ. Technol. Innov.* **2021**, *23*, 101524. [CrossRef]
35. *ASTM D95*; Standard Test Method for Water in Petroleum Products and Bituminous Materials by Distillation. ASTM International: West Conshohocken, PA, USA, 2018.
36. *ASTM D482*; Standard Test Method for Ash from Petroleum Products. ASTM International: West Conshohocken, PA, USA, 2019.
37. *ASTM D1298*; Standard Test Method for Density, Relative Density, or API Gravity of Crude Petroleum and Liquid Petroleum Products by Hydrometer Method. ASTM International: West Conshohocken, PA, USA, 2017.
38. *ASTM D97*; Standard Test Method for Pour Point of Petroleum Products. ASTM International: West Conshohocken, PA, USA, 2022.

39. *EN 12591*; Bitumen and Bituminous Binders. Specifications for Paving Grade Bitumens. European Committee for Standardization (CEN): Brussels, Belgium, 2009.
40. Gunka, V.; Bilushchak, H.; Prysiazhnyi, Y.; Demchuk, Y.; Hrynchuk, Y.; Sidun, I.; Shyshchak, O.; Bratychak, M. Production of Bitumen Modified with Low-Molecular Organic Compounds from Petroleum Residues.4. Determining the Optimal Conditions for Tar Modification with Formaldehyde and Properties of the Modified Products. *Chem. Chem. Technol.* **2022**, *16*, 142–149. [CrossRef]
41. *EN 1426*; Bitumen and Bituminous Binders. Determination of Needle Penetration. European Committee for Standardization (CEN): Brussels, Belgium, 2015.
42. *EN 1427*; Bitumen and Bituminous Binders. Determination of the Softening Point—Ring and Ball Method. European Committee for Standardization (CEN): Brussels, Belgium, 2015.
43. *DSTU 8825:2019*; Bitumen and Bituminous Binders. Determination of the Ductility. State Enterprise "Ukrainian Research and Training Center for Problems of Standardization, Certification and Quality": Kyiv, Ukraine, 2019.
44. *EN 12593*; Bitumen and Bituminous Binders. Determination of the Fraass Breaking Point. European Committee for Standardization (CEN): Brussels, Belgium, 2015.
45. *EN 12607-1*; Bitumen and Bituminous Binders. Determination of the Resistance to Hardening under the Influence of Heat and Air—Part 1: RTFOT Method. European Committee for Standardization (CEN): Brussels, Belgium, 2014.
46. Liang, M.; Ren, S.; Sun, C.; Zhang, J.; Jiang, H.; Yao, Z. Extruded tire crumb-rubber recycled polyethylene melt blend as asphalt composite additive for enhancing the performance of binder. *J. Mater. Civ. Eng.* **2020**, *32*, 04019373. [CrossRef]
47. Shpariy, M. Improvement of Ethylene Chlorination Technology. Ph.D. Thesis, Lviv Polytechnic National University, Lviv, Ukraine, 7 May 2021. Available online: https://lpnu.ua/sites/default/files/2021/dissertation/12197/shpariy-disertaciya.pdf (accessed on 5 April 2021).
48. *DSTU 8772:2018*; Mineral Filler for Asphalt Concrete Mixtures. Methods of Tests. State Enterprise "Ukrainian Research and Training Center for Problems of Standardization, Certification and Quality": Kyiv, Ukraine, 2018.
49. Parker, F. *Applications of Infrared Spectroscopy in Biochemistry, Biology, and Medicine*; Springer Science & Business Media: Berlin/Heidelberg, Germany, 2012.
50. *DSTU B B.2.7-127:2015*; Stone Mastic Road Concrete MIX and stone Mastic Asphalt. Specifications. State Enterprise "Ukrainian Research and Training Center for Problems of Standardization, Certification and Quality": Kyiv, Ukraine, 2015.